University of Groningen

3D visualization and analysis of HI in and around galaxies

Punzo, Davide

Link to publication in University of Groningen/UMCG research database

Chapter 1

Introduction

Since several decades, galaxy evolution has been one of the most important fields of research in astrophysics. There are at least two parameters that regulate the evolution of galaxies: their masses and their environment. In this introduction I summarize the understanding of regarding the influence of the gas component of the universe on these two parameters and the prospects for using upcoming large neutral hydrogen (H I) surveys from new and upgraded radio telescopes to improve this understanding. I will introduce my contribution to disclosing this information: a new visualization tool for the analysis of such data.

1.1 Hydrogen in galaxies

The contribution of baryonic matter to the total energy content of the universe, estimated from the current cosmological models, is about 4% (Planck Collaboration et al., 2016). Half of this is locked up in stars and the interstellar medium (ISM) in galaxies (Anderson and Bregman, 2010). The

rest resides in the intergalactic medium (IGM) which forms a cosmic web of gaseous filaments following the dark matter distribution in the universe (Crain et al., 2017). The dominant component of the interstellar and the intergalactic medium is hydrogen in its various states, i.e. neutral hydrogen (H I), ionized hydrogen (H II) and molecular hydrogen (H_2).

According to the hierarchical scenario of structure formation, galaxies form from the collapse of over-dense regions of matter (Springel et al., 2005; Vogelsberger et al., 2014; Schaye et al., 2015). The gas in the intergalactic medium is ionized and diffuse, i.e. a plasma of protons and electrons with a fraction of helium nuclei and traces of heavier elements. At these low densities, the gas undergoes continuous photo-ionization by the UV background and the time-scales for recombination are usually much longer than a Hubble time. Hydrogen, on the other hand, could be trapped in potential wells and confined in clouds at densities which are large enough to shield them from the ionizing radiation (Peebles, 1968; Arnaud and Rothenflug, 1985; Sutherland and Dopita, 1993; Haardt and Madau, 1996). In this case it can exist in a neutral, atomic and even molecular state and it becomes more susceptible to gravitational instabilities. Thus, gas clouds could collapse to form stars. Subsequent galaxies grow by accretion of smaller substructures of baryonic and dark matter (White and Rees, 1978). Physical properties of the collapsing gas, such as angular momentum, density and temperature, deeply affect morphologies and structural parameters of galaxies (Steinmetz and Navarro, 2002). Once collapsed, the gas constitutes the reservoir from which stars can form and the continuous acquisition of gaseous matter from the surrounding environment (e.g., cold accretion of gas from the cosmic web; see Section 1.4) guarantees the support of star formation for many billions of years.

One of the important tools to study galaxy evolution is the color–magnitude diagram. It provides information about how absolute magnitude and mass of galaxies are related (see Fig. 1.1). A preliminary description of the three areas (red, blue and green) of this diagram was given by Bell et al. (2003) using the COMBO-17 survey, which revealed the bimodal distribution of red and blue galaxies.

The three galaxy families shown in Fig. 1.1 have different characteristics and properties which are related to the environment, the age and the formation history (for a detailed review see e.g. Baldry et al., 2004, 2006; Kauffmann et al., 2004). The so-called *red-sequence* galaxies are associated with *early* type galaxies which are elliptically-shaped, have low dust and
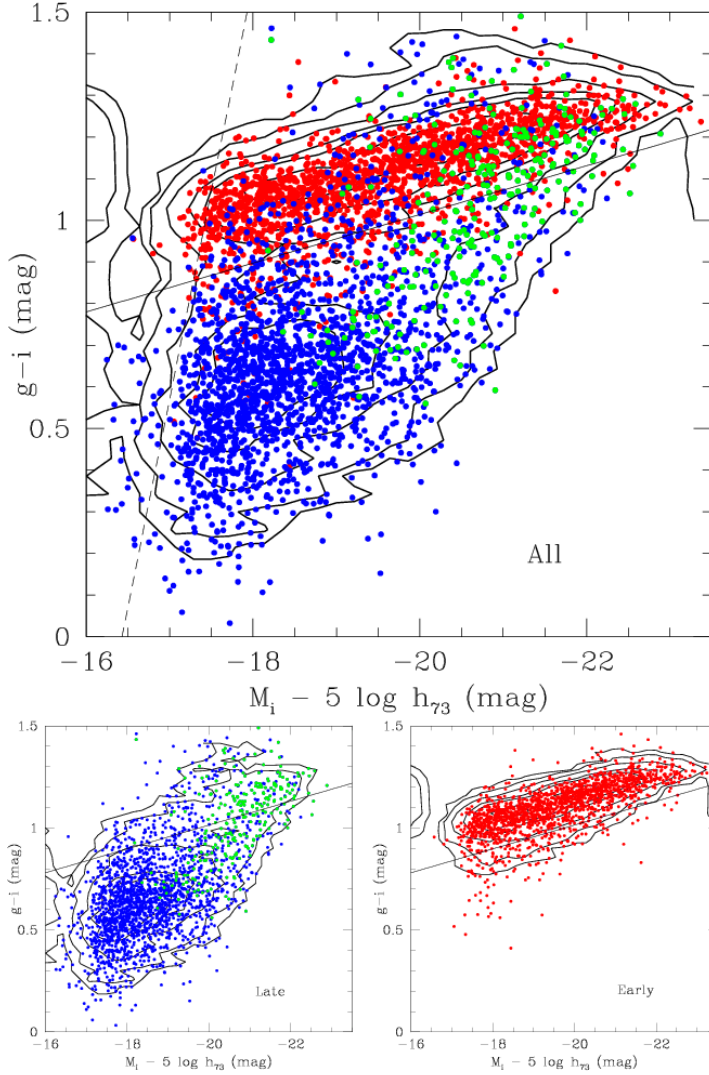
Figure 1.1 – $g-i$ color versus i-band absolute magnitude relation of all galaxies in the CS coded according to Hubble type: red = early-type galaxies (dE-E-S0-S0a); blue = disk galaxies (Sbc-Im-BCD); green = bulge galaxies (Sa-Sb): all galaxies (top); late-type from Sa to Im-BCD (bottom left); early type (bottom right). Contours of equal density are given. The continuum line $g-i = -0.0585*(Mi+16)+0.78$ represents the empirical separation between the red-sequence and the remaining galaxies. Figure from Gavazzi et al. (2010).

gas contents, and are dominated by old and red stars. The *blue-sequence* or the *blue-cloud* galaxies are associated with *late* type galaxies which usually have disk-like structures with spiral arms, large amounts of gas and dust and young stellar populations. The third family is called the *green valley.* The properties of these objects are still under investigation. The green valley can be a transitory phase of galaxies shifting from the blue sequence to the red one (Salim, 2014; Genel et al., 2014; Trayford et al., 2016).

To fully understand the build up of stellar mass in galaxies, it is necessary to identify also the role of the gas, the fuel for star formation, together with the physical processes governing the evolution of galaxies. In this thesis, the focus is on the neutral atomic component, the H I, in (and around) disk galaxies, which can be observed with radio telescopes through its 21-cm emission-line. The radio emission-line at 21-cm from neutral hydrogen was theoretically predicted by van de Hulst (1944) and was first detected in the Milky Way by Ewen and Purcell (1951) and confirmed by Muller and Oort (1951). The 21-cm line arises from a transition between the hyper-fine structure levels in the ground state of atomic hydrogen. This results from magnetic interactions between the quantized electron and proton spins and it can be detected both in emission and absorption. Moreover this radiation does not interact with interstellar dust, making the 21 cm line almost extinction-free (it can still suffer from absorption when it interacts with hydrogen atoms). Half a century of observations of neutral hydrogen of many gas-rich galaxies at low redshift ($z \lesssim 0.2$) have provided a wealth of information on the distribution of gas, the kinematics and the dynamics of disk galaxies.

1.2   H I and kinematics of galaxies

The study of the kinematics of galaxies is a very important probe for studying their gravitational potential. Most stars and gas in spiral galaxies reside in a disk-like structure, but the detectable H I disks usually extend much farther out than the stellar ones and can reach radii 2-3 times greater than the stellar disks. A comparison between the optical image and the integrated H I image for the spiral galaxy NGC6946 (Boomsma et al., 2008) is shown in Fig. 1.2 as an illustration.

In this context, neutral hydrogen is a unique tool for studying the kinematics of spiral galaxies on a large scale. A classical example is the discovery of dark matter: in the 1970s, thanks to H I observations,
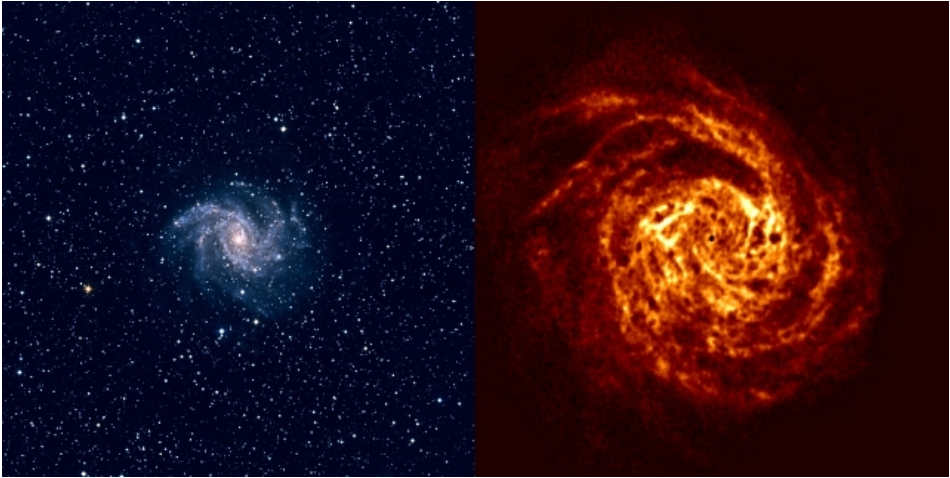
Figure 1.2 – Comparison between the optical image (left) and the total H I image (right) for thespiral galaxy NGC6946 from Boomsma et al. (2008). Images have the same scale.

astronomers realized that the rotation curves of spiral galaxies, i.e. the variation in the orbital circular velocity as a function of radius, remain high at large distances from the center, higher than expected considering the distribution of visible matter (Bosma, 1978; van Albada et al., 1985). A constant velocity with increasing radius implies that the mass must be increasing linearly with radius, while the observed visible mass usually falls off exponentially beyond a characteristic radius. This evidence led astronomers to postulate the presence of an unknown and undetectable kind of matter which did not interact with radiation, hence named *dark matter*. Subsequently, using H I detailed rotation curves it became possible to model the distribution, the density profile and the gravitational potential of dark matter haloes (Bosma, 1981; Kent, 1987; Walter et al., 2008a).

1.3   H I content and star formation rate in galaxies

The field of H I research includes the study of the empirical relation between the gas density and star formation rate (SFR). The relation was first examined by Schmidt (1959). In his paper he derived and proposed a model, assuming a time-independent initial mass function, in which the SFR volume density is proportional to the local gas volume density. He investigated the properties of the star formation comparing
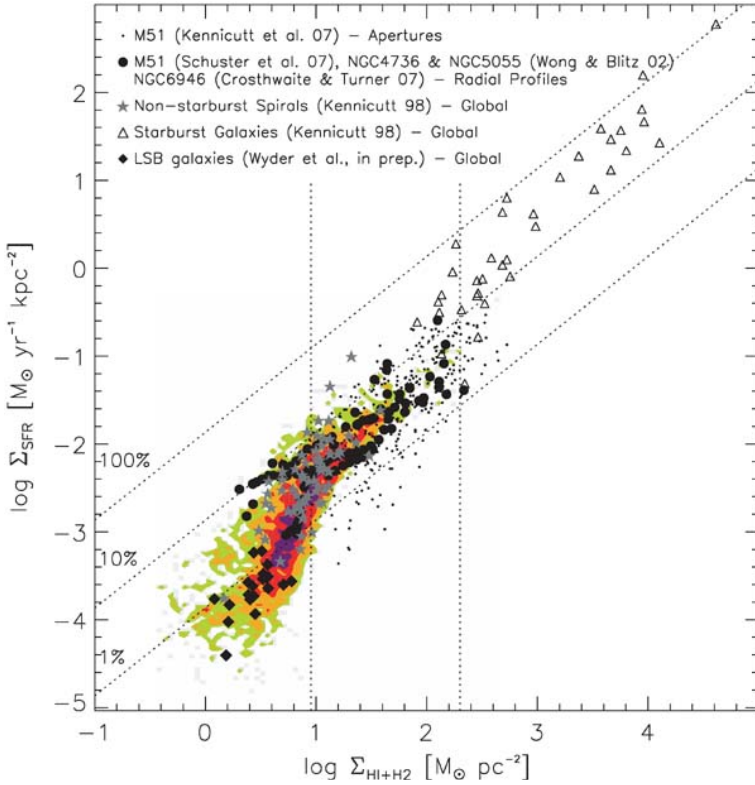
Figure 1.3 – Σ_{SFR} vs. Σ_{gas} compilation of different studies by Bigiel et al. (2008). Colored contours show the data from Bigiel et al. (2008). Plotted as black dots are data from measurements in individual apertures in M51 (Kennicutt et al., 2007). Data points from radial profiles from M51 (Schuster et al., 2007), NGC4736, and NG5055 (Wong and Blitz, 2002) and from NGC6946 (Crosthwaite and Turner, 2007) are shown as black filled circles. In this figure disk-averaged measurements from 61 normal spiral galaxies (filled gray stars) and 36 starburst galaxies (triangles) from Kennicutt (1998a) are shown as well. The black filled diamonds show global measurements from 20 low surface brightness galaxies (Wyder et al., 2009). There is a good qualitative agreement between the measurements despite the variety of SFR tracers that have been used. This summary figure clearly shows three distinctly different regimes (indicated by the vertical lines) for the SF law.

and constraining the proposed model with observations of the distribution of the gas and young stars in the solar neighborhood. He concluded that the best fit with the observations is given by a model in which the SFR varies with the square of the gas density.

At the end of 1990s, Kennicutt (1998a,b) established that the value of the parameter n in the relation between the local SFR surface density, Σ_{SFR}, and the local gas surface density, Σ_{gas}, i.e.:

$$\Sigma_{SFR}(M_\odot \ yr^{-1} \ kpc^{-2}) \propto \Sigma_{gas}^n(M_\odot \ pc^{-2}), \tag{1.1}$$

is less than 2. The analysis was performed both for 61 normal disk galaxies and 36 infrared-selected circumnuclear starbursts. The results were $n = 1.4 \pm 0.13$ for the first case and $n = 1.28 \pm 0.08$ for the second one. More recent work shows that the value n is 1.0 ± 0.2 for regions with high gas density and up to 2.5 for lower density regions as shown in Fig. 1.3 (see Bigiel et al., 2008).

One of the main puzzles in galaxy evolution is that the rate at which new stars have formed in galaxies has declined dramatically over the last 7 Gyr (e.g., Madau et al., 1998; Hopkins and Beacom, 2006), while the density of cold gas in the universe, Ω_{GAS}, remains almost constant (Lah et al., 2007). Fig. 1.4 shows the trends of the cosmic SFR density and the cosmic gas density with redshift.

Observed star formation rates in galaxies are such that the observed gas supply is exhausted in a few Gyr (e.g., Bigiel et al., 2008) and the dwindling star formation could, in principle, be due to star formation consuming the available gas supply. Instead the total amount of gas observed in the galaxies decreases at most by a factor 2 during the recent evolution of the universe as showed in Fig. 1.4.

Galaxies must, therefore, continuously accrete gas from the intergalactic environment to sustain the observed gas density levels. A fraction of this gas is of extragalactic origin (Sancisi et al., 2008). Sancisi et al. (2008) have pointed out that there is a mean "visible" accretion rate of cold gas in galaxies of at least 0.2 $M_\odot$/yr (i.e., cold accretion from the cosmic web). In order to reach the accretion rates needed to sustain the observed star formation ($\sim 1.0 \ M_\odot$/yr), additional infall of large amounts of gas from the IGM would be required.

Models of galactic fountains (Bregman, 1980; Marinacci et al., 2011; Marasco et al., 2013), offer a solution in which nearly $20 - 30 \ M_\odot$/yr of cold gas clouds are expelled from the host galaxy by events, like supernovae,
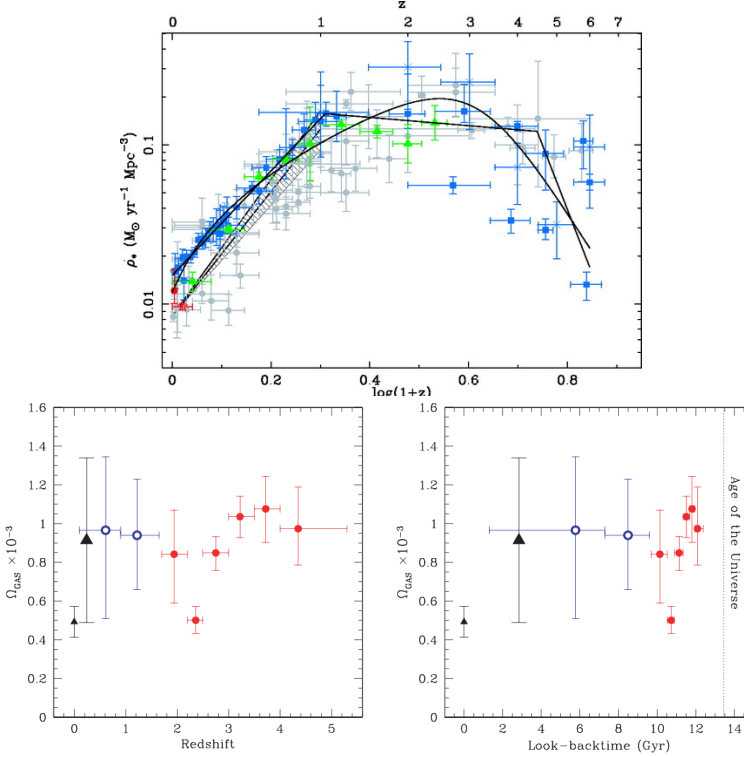
Figure 1.4 – The top panel shows the evolution of SFR density as a function of redshift as presented by Hopkins and Beacom (2006). The gray points are from the compilation of Hopkins (2004). The hatched region is the FIR (24 m) SFH from Le Floc'h et al. (2005). The green triangles are FIR (24 m) data from Pérez-González et al. (2005). The open red star at z = 0.05 is based on radio (1.4 GHz) data from Mauch (2005). The filled red circle at z = 0.01 is the H I estimate from Hanish et al. (2006). The blue squares are UV data from Baldry et al. (2005), Wolf et al. (2003), Arnouts et al. (2005), Bouwens et al. (2003b), Bouwens et al. (2003a), Bouwens et al. (2005), Bunker et al. (2004), and Ouchi et al. (2004). The blue crosses are the UDF estimates from Thompson et al. (2006). Note that these have been scaled to the SalA IMF, assuming they were originally estimated using a uniform Salpeter IMF. The solid lines are the best-fitting parametric forms. The bottom figures show the neutral gas density of the universe as a function of redshift and look-back time (Lah et al., 2007). The small triangle at $z = 0$ is the HIPASS 21-cm emission measurement from Zwaan et al. (2005). The filled circles are damped $Ly\alpha$ measurements from Prochaska et al. (2005). The open circles are damped $Ly\alpha$ measurements from Rao et al. (2006) using HST. The large triangle at $z = 0.24$ is our H I 21-cm emission measurement made using the GMRT. All results have been corrected to the same cosmology and include an adjustment for neutral helium.

but will not reach the escape velocity. After a timescale of 100 Myr, these clouds fall back into the galaxy bringing with them ~ 2 $M_\odot$/yr of gas extracted from the hot halo (i.e., accretion from the galaxy halo).

1.4   H I signatures of gas accretion and removal

The importance of gas accretion and removal processes in galaxies is still unclear: continuous accretion of gas can definitely solve the gas discrepancy so that star formation can continue over much longer periods than supported by the initial gas reservoirs and gas consumption times. Conversely, the study of physical processes that remove gas such as the feedback from star formation and from an AGN (active galactic nucleus) is also crucial (Kereš et al., 2009). Other effects can also remove gas from galaxies, such as tidal interactions and, in the hot intergalactic medium in clusters of galaxies, ram-pressure stripping (Sancisi et al., 2008).

H I can probe these processes and can provide information regarding the environment around galaxies. For example, H I is an excellent tool to investigate tidal interactions. Ongoing major and minor interactions can lead to traumatic mergers or to accretion and trigger star formation. These events show distinct H I signatures. Examples of H I tidal tails are shown in Chapters 2, 3 and 4. Sancisi (1999) estimated that up to 50% of the galaxies in very high density regions have been through tidal interactions in their history. Such interactions can provide a mean accretion rate for gas up to 0.5 $M_\odot$/yr.

Moreover, evidence for the accretion of cold gas in galaxies has been rapidly accumulating in the past years. H I observations of galaxies and their environment have brought to light new facts and phenomena which are evidence of ongoing or recent accretion (Sancisi et al., 2008):

1. A large number of galaxies have gas-rich dwarfs companion or are surrounded by complexes of H I clouds, tails and filaments. This suggests ongoing minor mergers and provides galaxies with external gas. This may be regarded as direct evidence of cold gas accretion from the cosmic web in the local universe.

2. Many nearby spiral galaxies show signatures of extra-planar H I. This gas can be produced by galactic fountains, but it is likely that a part of it is of extragalactic origin.
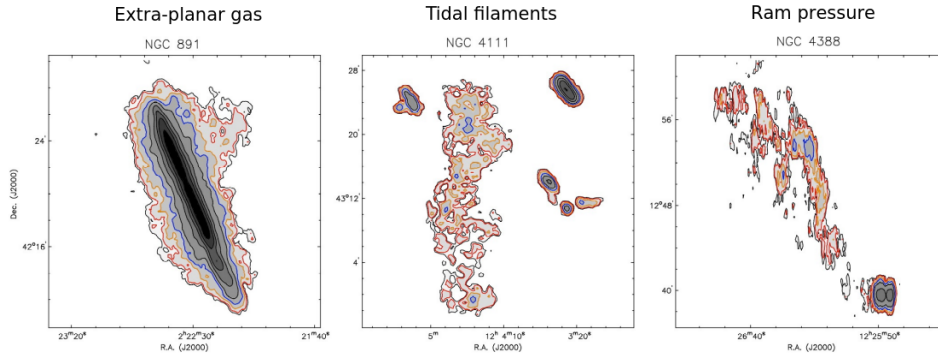
Figure 1.5 – Three examples of very faint (unusual) H I emission around galaxies. The left panel shows the presence of extra-planar gas (Oosterloo et al., 2007). The central panel shows a group of galaxies and a very faint tidal filament between them (Verheijen and Zwaan, 2001). The right panel highlights a long filament due to ram-pressure stripping (Oosterloo and van Gorkom, 2005). The column density contours are at levels of 2×10^{19} cm^{-2} (red), 5×10^{19} cm^{-2} (orange) and 1×10^{20} (blue) cm^{-2}. Image credit M. Verheijen.

3. Spirals have extended and warped outer layers of H I. The kinematic formation and evolution of these is not clear. One hypothesis is that they are the consequences of gas infall from the cosmic web into the galaxy.

4. The majority of galactic disks are lopsided in their morphology as well as in their kinematics (i.e., they are not symmetric). Also here recent accretion has been advocated as a possible cause.

Two crucial elements for obtaining the full picture of galaxy evolution are: i) characterizing the star formation properties and stellar populations as has become possible though dedicated surveys such as the Sloan Digital Sky Survey; ii) understanding the detailed balance between gas accretion and gas depletion removal processes and how they depend on the environment. Examples of observations that have detected H I associated with such processes are shown in Fig. 1.5. A full inventory of these in a well defined volume in the nearby universe is needed to complement the wealth of optical and near-IR data.

1.5   H I surveys

Upcoming blind H I surveys such as WALLABY, using the ASKAP telescope (Johnston et al., 2008; Duffy et al., 2012), the shallow and medium-deep Apertif surveys, using the WSRT telescope (Verheijen et al., 2009, `www.apertif.nl`), and future surveys with the Square Kilometre Array, SKA, are designed to answer the following key questions related to the role of H I in galaxies:

1. What are the distribution and kinematics of the neutral (H I) gas within and around galaxies, both as a function of environment (i.e., groups/clusters vs. the field) and over cosmic time?

2. What is the cosmic H I density as a function of redshift?

3. How does the $M_{H I}$ of galaxies scale with their stellar/halo masses and other properties, e.g., star formation rate, as a function of environment and redshift?

4. How important is gas accretion compared to merging in terms of building up stellar mass?

One of the goals of Apertif will be a blind survey of a few hundred $\deg^2$ with high sensitivity reaching a column density depth of 3×10^{19} cm^{-2}. This will allow an inventory of the dominant gas acquisition and gas removal processes in at least a few thousand galaxies in different environments.

Therefore, Apertif (and other SKA precursors) will deliver an unprecedented amount of data. Each day Apertif will provide a data-cube of size ~ 1 TByte containing about one hundred galaxies. This expected steep increase in data volume from both the increased field of view ($\sim 30\times$) and bandwidth ($\sim 10\times$) has created the necessity of automated tools for calibration and finding the sources. Automatic pipelines will become a necessity to handle the analysis of these large datasets.

However, the H I signatures of gas accretion and removal (i.e., H I tails, filaments and extra-planar gas) usually have very low column density and are very faint (signal-to-noise ratio ~ 1). In addition, their signature can be very subtle and hard to separate from the rest of the data and, therefore, these objects are easily missed by automated pipelines. Therefore, manual inspection and visualization of the sources will still play a major role for finding such features in the results generated by the pipelines and will assist in their detailed analysis.

1.6   The role of 3D visualization

Traditionally visualization in radio astronomy has been used for:

1. finding artifacts due to an imperfect reduction of the data;

2. finding sources and qualitatively inspect them;

3. performing quantitative and comparative analysis of the sources.

3D *Large* visualization algorithms (e.g., Hassan et al., 2013) and tools (e.g., Vohl et al., 2016) can provide full 3D navigation around very large data-cubes (~ 1 TByte) and/or efficient display of many small cubelets ($\lesssim 1$ GByte) that surveys will provide, boosting the exploration of the data. These techniques can help and improve the process of inspecting large data-cubes for the identification of artifacts (e.g. Radio Frequency Interference, RFI) and H I emission from galaxies (sources), but they are demanding in terms of hardware resources (see Chapter 2). Therefore, in this thesis we mainly investigate how to enhance the manual inspection of the individual sources delivered by automated pipelines (i.e., cubelets around sources, masks and models) and in particular the inspection and analysis of complex cases, using interactive 3D visualization tools and analysis techniques running on systems with limited resources (i.e., software solutions aimed at desktops/laptops).

Apertif will most likely deliver 2 or 3 morphologically and/or kinematically complex cases every day (see Chapter 2 for more information). The subcubes containing these sources will be relatively small with maximum sizes of $512 \times 512 \times 256 \sim 67$ Megavoxels, reducing the local storage, I/O bandwidth, and computational demand for visualization (easily achievable on a modern computer). On the other hand, powerful Visual Analytics (i.e., coupling of interactive visualization with analysis routines to support and enhance the manual inspection of the data; see also Section 2.2.6) tools will be necessary to enhance the inspection and analysis of the several thousand galaxies that the blind surveys will provide in few years. Coupling visualization tools with semi-automated data analysis techniques will be a very powerful way to improve the inspection itself.

In the mid-1990's, Oosterloo (1995) demonstrated the benefits (and drawbacks) of volume rendering algorithms for visualizing the 21-cm radio emission of galaxies (a more detailed discussion is provided in Chapter 2). For example, In Fig. 1.6, the three-dimensional visualization of a particular
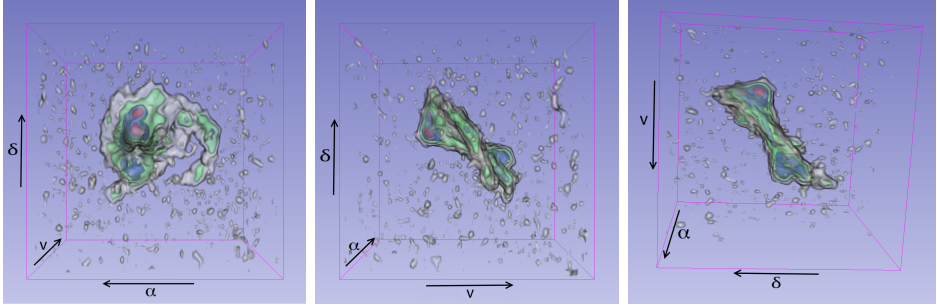
Figure 1.6 – Three views of the volume rendering of a particular source in the PPScl filament (data from Ramatsoku et al., 2016) are shown. In the left panel we look along the velocity axis; in the central panel along the RA axis; and int the right the view is parallel to the geometrical major axis of the galaxy. The different colors highlight different intensity levels in the data (i.e., grey, green, blue and red correspond to 3, 8, 15 and 20 times the rms noise respectively).

source in the the Perseus-Pisces Supercluster (PPScl) filament, discussed in section 2.3, shows a 3D view of its H I distribution and kinematics. Two main components are visible in Fig. 1.6: a central body, which is the regularly rotating disk of the galaxy, and a tail which is unsettled gas resulting from tidal interaction with another galaxy. 3D visualization provides an immediate overview of the coherence of the data in the spatial and velocity dimensions.

At the time, Norris (1994) defined two main requirements to effectively use 3D visualization for studying H I sources: interactive performance and quantitative capabilities. However, the use of full 3D (i.e. volume rendering) visualization of H I in galaxies is still in its infancy. Existing astronomical 3D visualization tools indeed cannot perform interactive 3D navigation in the data and/or interactively change the color/opacity functions used to render the data. Moreover, they also lack analysis tools integrated with the visualization which provides powerful quantitative and comparative visualization capabilities to the tool itself (see Chapter 4 for more details). The lack of interactivity is mainly a result of the lack of computing power to date, as volume rendering is computationally expensive (when the existing software was developed massive parallel hardware was not available in personal computers). Moreover, the use of 2D input and output hardware limits the interaction with a 3D representation (e.g. performing a 3D selection of the data; see Section 2.2.5). An additional complication is

that the 3D structure of the H I in a cube is not in a 3D spatial domain. The third axis represents velocity and thus the 3D rendering delivers a mix of morphological, kinematical and geometrical information. These are the main reasons why the development of 3D visualization as a tool for inspecting, understanding and analyzing radio-astronomical data has been slow.

Currently available hardware, in particular *Graphic Processing Units* (GPUs), enables interactive volume rendering, stimulating further development. In addition, the interoperability between 2D visual representations (e.g. channel movies and position-velocity diagrams) and 3D visualization techniques (volume rendering) of 3D data is a key capability which will enhance the exploration of 3D astronomical data. 3D visualization is not a replacement of 2D visual representations, but each one enhances the other: 3D provides an immediate overview of the structure in the data, while in 2D representations is easier to interact "pixel by pixel" with the data.

1.7   This thesis

In this thesis I investigate state-of-the-art techniques for interactive 3D visualization, 3D filtering and 3D selection to boost the inspection and analysis, in terms of both efficiency and quality, of complex sources with faint and subtle components. For testing a variety of volume rendering, smoothing and selection algorithms, I used a test sample of H I data-cubes. These datasets show complex H I structures such as tidal-tails (e.g., WEIN069), filaments (NGC4111) and extra-planar gas (NGC2403). These extremely faint components are currently hardly separable from the noise, but coherent in the 3D space (two spatial dimensions and one velocity dimension). Developing techniques to identify, inspect and analyze them is of primary importance to study all aspects of the H I in and around galaxies.

In more details, I investigate algorithms and new software package solutions to solve the following visualization and analysis problems:

(A) How to boost the inspection of many complex H I sources?

The planned H I blind surveys will provide thousands of sources that will show a complex nature (see Chapter 2 and Sancisi et al., 2008). In such cases manual inspection will definitively be required as the automated pipelines will have trouble characterizing complex cases. The current

visualization tools used in astronomy will however not suffice anymore. Current available 2D visualization tools for 3D astronomical data are powerful, but they lack the *interactive* volume rendering capabilities that can provide a much faster overview of all coherences in the data.

(B) How to efficiently find faint H I structures such as filaments and tidal tails?

Current astronomical visualization tools require that the user properly modifies the color function of the 2D display and navigates through many slices in the data-cube in order to find the very faint emission. Such an approach is not efficient because the user has to perform many interactions and navigate through the data-cube using 2D visual representations and must remember each visual representation. Full 3D volume rendering of the data and flexible visualization can greatly improve this situation and is explored in this thesis.

(C) How to perform visual analytics tasks in the 3D environment?

Visual analytics, i.e. the combination of human reasoning and judgment with automated data processing supported by interactive visualization, is of primary importance for enhancing the manual analysis of complex galaxies. However, 3D selection tools to choose a region of interest (ROI) in the 3D space are not available in the current astronomical software packages, so the development of such a capability is badly needed and is part of this project.

(D) How to enhance the identification and inspection of subtle gas components in galaxies such as extra-planar gas?

The H I emission from galaxies usually consists of a regularly rotating cold disk (i.e. in differential rotation) and subtle faint gas components such extra-planar gas. The latter has different kinematical properties from the disk, but it is not straightforward to identify them by only visualizing the data.

In addition, although the main focus of the thesis is on 3D H I data, the techniques and the software developed in this thesis are useful for other types of 3D data such as and mm/submm molecular line data and optical

integral field spectroscopic data. However, such applications will require more research and development of tools tailored to the kind of data and the scientific questions to be addressed (see Chapters 4 and 5) and are not addressed further in this thesis.

1.7.1   Thesis outline

The structure of this Ph.D. thesis is as follows:

In Chapter 2, I present data samples of Apertif-like observations and I produce 3D representations of such data. Moreover, I explore in detail the 3D signatures and structures of H I data and the advantages in showing such data with *interactive* 3D visual representations, as partially already pointed out by Oosterloo (1995). Finally, I formulate the requirements for visualizing them and I review the state-of-the-art of rendering algorithms and scientific visualization software packages.

In Chapter 3, using H I data from a variety of galaxies, I explore state-of-the-art filtering algorithms and how to employ them in an interactive 3D visualization environment to find faint and complex structures such as tidal tails and filaments. In this chapter, I investigate several 3D smoothing and thresholding state-of-art techniques. I find that an optimal algorithm exists which preserves the high signal-to-noise data while smoothing only the very faint data, while requiring only minimal tuning of the input parameters.

In Chapter 4, I investigate how to enhance the analysis of H I emission from galaxies in the context of a 3D environment. First, I introduce the `CloudLasso` selection tool (Yu et al., 2012). This is a 3D interactive tool to choose regions of interest (ROI) in 3D visual representations. The tool is powerful, because it combines volume rendering (which enables an immediate overview of all the structures in the data) with the human decision-making: the user can navigate in the 3D space, find the optimal 3D view and perform a selection in the 3D space of the structures visible in the 3D view. Therefore, `CloudLasso` is an intuitive and efficient 3D selection method, which is crucial for creating (or modifying) ROI in the 3D space. Second, we investigate how to use automated tilted-ring modeling fitting software (e.g., Di Teodoro and Fraternali, 2015b) which fits only the symmetric, regularly rotating gas disks of galaxies, to separate and visually highlight the data fitted by the modeled disk from unusual H I components such as extra-planar-gas. In particular, I investigate how to efficiently visualize the model and the data in the full 3D environment to

provide an enhanced overview of the different kinematical components in galaxies.

In Chapter 4, I also present `SlicerAstro`. With `SlicerAstro`, an extension of `3DSlicer` (version 4), a multi-platform package for visualization and medical image processing, I aim to provide a 3D interactive viewer with new analysis capabilities, based on traditional 2D input/output hardware, for astronomical 3D datasets. Borkin et al. (2005, 2007) conducted a similar investigation of medical imaging software including `3DSlicer`. They also found that volume rendering and segmentation techniques can enhance the inspection of astronomical datasets. However, they could not extend `3DSlicer` (version 3 at that time) to provide the capabilites (e.g., integration of astronomical world coordinates systems, filtering and 3D selection) I implemented in the current version of `3DSlicer`.

Finally, in Chapter 5, I present a summary of the thesis and I list the potential future developments of `SlicerAstro`.